PHYSICAL REVIEW A **82**, 011401(R) (2010)

Observation of vibration-dependent electron anisotropy in O_2^- photodetachment

Richard Mabbs, Foster Mbaiwa, Jie Wei, and Matthew Van Duzor
Department of Chemistry, Washington University in St. Louis, Campus Box 1134, Saint Louis, Missouri 63130, USA

Stephen T. Gibson, Steven J. Cavanagh, and Brenton R. Lewis
Research School of Physics and Engineering, The Australian National University, Canberra ACT 0200, Australia
(Received 20 March 2010; published 2 July 2010)

Photoelectron angular distributions (PADs) recorded for the $O_2(X\,^3\Sigma_g^-) \leftarrow O_2^-(X\,^2\Pi_g)$ band show significant vibrational dependence. Experimental evidence of vibrational influence on the PAD has, to date, been sparse. Consequently, little attention has been paid to vibrational effects in the consideration of direct detachment processes by recent theoretical treatments. The results presented here demonstrate the sensitivity of the PAD to vibronic coupling in the anion ground electronic state, a phenomenon which is usually neglected in direct molecular anion photodetachment. These results provide the essential data for the evaluation and refinement of existing theoretical models.

DOI: 10.1103/PhysRevA.82.011401 PACS number(s): 33.80.Eh

The photoelectron differential cross section ($d\sigma/d\Omega$), characterized by the anisotropy parameter $\beta(E)$, is a sensitive probe of anion photodetachment dynamics and electronic structure, representing the signature of the parent anion orbital in the atomic case [1]. The use of $\beta(E)$ as a diagnostic of a parent atomic orbital is complicated by an electron kinetic energy (E) dependence. However, atomic anion direct detachment experiments varying the photon energy ($h\nu$) show that the $\beta(E)$ values lie on a single, smooth curve for a given electronic transition [2,3]. Conservation of energy links $h\nu$ and E: $h\nu = E + \text{eBE}$, where eBE is the electron binding energy. For molecular anion direct detachment, $\beta(E)$ predictions usually ignore the effects of internal excitation (even for diatomics). In the absence of vibrationally resolved experimental data, the approximation that $I(E,\theta)$ depends solely on the parent orbital is usually employed. $\beta(E)$, therefore, should be the same for a given E, regardless of $h\nu$ and vibrational energy change.

We present detailed experimental measurements of the $\beta(E)$ values associated with the $O_2(X\,^3\Sigma_g^-, v') \leftarrow O_2^-(X\,^2\Pi_g, v'' = 0)$ band, in particular examining the role of vibrational degrees of freedom which demonstrate this assumption to be overly simplistic. $\beta(E)$ dependence on internal degrees of freedom has been seen previously in indirect ionization processes [4,5]. The current results clearly show that internal excitation can have a significant effect, even for direct photodetachment. These data will serve as stimuli for future theoretical developments and provoke similar investigation of other electronic transitions in diatomic and polyatomic molecular anions.

Linearly polarized photons yield a photoelectron angular distribution (PAD) equivalent to $d\sigma/d\Omega$ and described by:

$$I(E,\theta) = \frac{\sigma(E)}{4\pi}[1 + \beta(E)P_2(\cos\theta)], \qquad (1)$$

where $P_2(\cos\theta)$ is the second Legendre polynomial, and θ is the angle between the laser electric vector, $\boldsymbol{\varepsilon}_\mathbf{p}$, and the photoelectron momentum, $\mathbf{k}$.

The photon energy dependence of the total detachment cross section [6–13], and the photoelectron spectrum of O_2^- [14–25] have been thoroughly characterized. However, much fewer data exist regarding the angular distribution [15,22]. This is surprising as O_2^- is an excellent candidate to study the vibronic effects on $I(E,\theta)$. The strong resemblance of the π_g molecular orbital to an atomic d orbital retains a link with atomic-anion detachment models. Additionally, the single vibrational mode has a high-enough frequency to allow the resolution of vibrational structure in the photoelectron spectrum.

Examination of the effect of vibrational motion on the PAD requires measurements over a range of E for several vibronic transitions. Such studies are rarely performed. Here, we employ a combination of velocity mapped imaging [26] and readily tunable, linearly polarized photon sources, allowing efficient accumulation of the necessary data.

The representative image shown in Fig. 1 is the result of 454.57 nm detachment of O_2^- using a high resolution ($\Delta E/E = 0.4\%$ or better), in-line imaging system. The image is a 2D projection of the 3D laboratory-frame-momentum-space photoelectron spectrum. Transitions associated with lower eBE are found at larger radii, which correspond to higher linear momentum. The rings in the image correspond to different vibronic transitions, and several electronic bands are present. For the sake of brevity, we focus on the outermost transitions, those associated with the $O_2(X^3\Sigma_g^-, v') \leftarrow O_2^-(X\,^2\Pi_g, v'' = 0)$ band.

To recover the original, cylindrically symmetric 3D distribution we apply an inverse Abel transformation to the image [27]. It is then possible to extract the PAD corresponding to a particular vibronic transition by integrating across the appropriate radial range at all θ and fitting Eq. (1) to the data using $\beta(E)$ as the fitting parameter. $\beta(E)$ values are very sensitive to experimental factors such as background noise and image distortion. To verify the observed trends, two independent sets of data are represented in this work, recorded on two different instruments at several wavelengths between 900 and 440 nm. The first set (Fig. 2, closed circles) was recorded on the high-resolution instrument using a Nd:YAG (Continuum Powerlite 9010) pumped OPO (Continuum Sunlite) laser, while a second set (Fig. 2, open circles) was recorded using a perpendicular imaging arrangement ($\Delta E/E = 10\%$) and Nd:YAG (Spectra Physics INDI-40–10-HG) pumped dye laser (Spectra-Physics

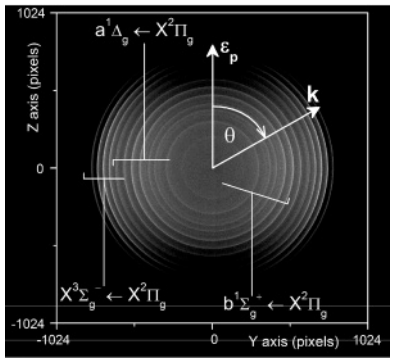

FIG. 1. Photoelectron image of O_2^- detachment at 454.57 nm.

Cobra Stretch). Details of both instruments can be found in Refs. [28] and [29], respectively. Although there is slightly greater scatter in the lower resolution measurements, the two sets are in excellent agreement. However, due to overlapping transitions in the lower resolution data, direct comparison is only possible for the O_2 ($X\,^3\Sigma_g^-$, $v' = 1$–4) $\leftarrow$ O_2^-($X\,^2\Pi_g$, $v'' = 0$) transitions shown in Figs. 2(a)–2(d).

The dominant centrifugal term in the anion potential results in significant E dependence of $d\sigma/d\Omega$ and the integral cross section σ [30–32]. This is clearly seen in the data in Fig. 2. Qualitatively similar trends are seen for each vibronic transition, with $\beta(E)$ becoming increasingly negative as E increases. To understand this behavior, we first return to atomic anion detachment.

Under the one-electron approximation, an atomic anion orbital is a central potential eigenfunction (specified by quantum number, ℓ). The photoelectron wave function can be expanded into a series of such eigenfunctions. Selection rules restrict the superposition to functions specified by $\Delta\ell = \pm 1$ [32–34]. Interference between these partial waves determines $\beta(E)$, and so the cross sections ($\sigma_{\ell\pm1}$) and phase difference [$\delta_{(\ell+1)-(\ell-1)}$] are critical [35]:

$$\beta(E) = \frac{\ell(\ell-1) + (\ell+1)(\ell+2)A^2E^2 - \ell(\ell+1)AE\cos\delta_{(\ell+1)-(\ell-1)}}{(2\ell+1)[\ell + (\ell+1)A^2E^2]}, \tag{2}$$

where A is related to anion size [35], and AE represents the ratio of the partial wave cross sections, $\sigma_{(\ell+1)}/\sigma_{(\ell-1)}$, assuming Wigner threshold behavior [31] is a valid approximation.

Molecular anion orbitals are not usually eigenfunctions of a central potential Hamiltonian. Furthermore, internal degrees of freedom may become important. In the spirit of Eq. (2),

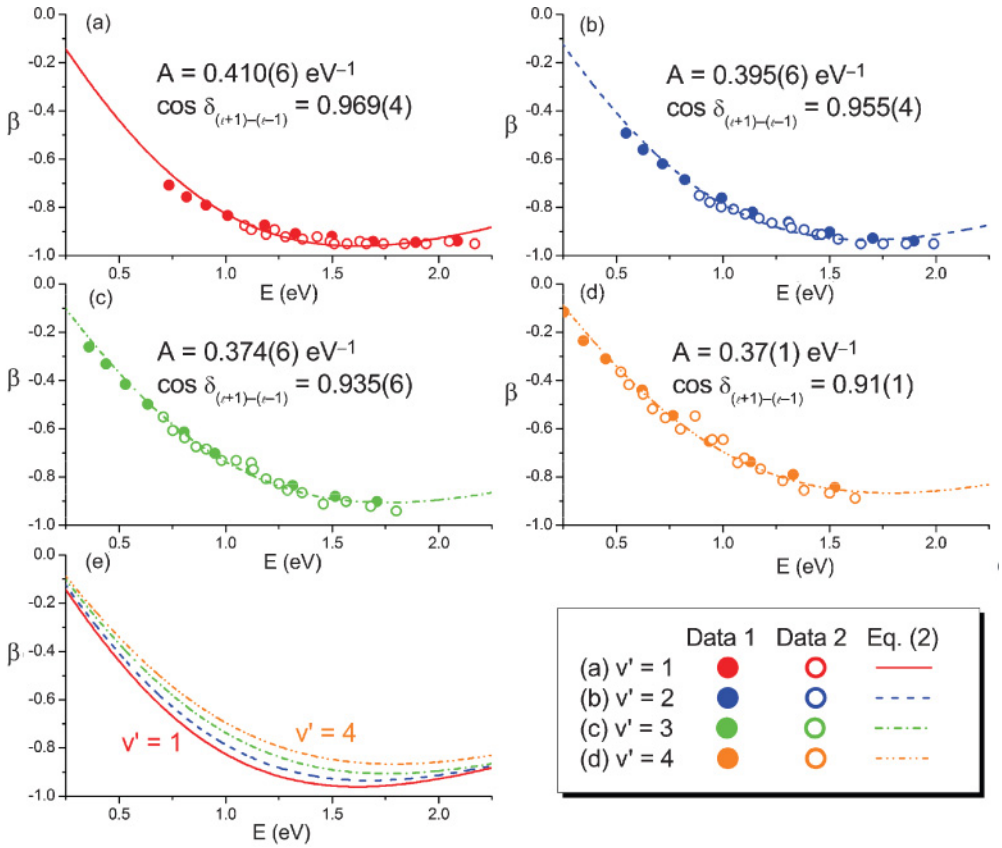

FIG. 2. (Color online) β parameters associated with each vibrational transition associated with the $O_2(X\,^3\Sigma_g^-, v') \leftarrow O_2^-(X\,^2\Pi_g, v'' = 0)$ band. (a) $v' = 1$, (b) $v' = 2$, (c) $v' = 3$, (d) $v' = 4$. Each point represents a different detachment wavelength. The curves are the result of fitting Eq. (2) to the data. The fitted curves are compared in (e).

anion detachment calculations tend to focus on the nature of the parent orbital itself. Although Eq. (2) applies strictly only to atomic anion detachment, fitting the atomic model to the data in Fig. 2 is instructive. The curves in Fig. 2 are obtained using A and $\cos\,\delta_{(\ell+1)-(\ell-1)}$ as fitting parameters and setting $\ell = 2$. The fits are generally very good (the adjusted coefficient of determination is >0.96 for $v' = 2$–4 and >0.86 for $v' = 1$) but, as summarized in Fig. 2, require different parameters for each vibronic transition. Both A and $\cos\delta_{(\ell+1)-(\ell-1)}$ decrease as v' increases. In practical terms this results from the v' dependence of the $\beta(E)$ trends, as seen in the comparison of the fits in Fig. 2(e).

The atomic picture of detachment (at least in terms of the electronic orbital) is a reasonable first approximation that reproduces the essential trends in the data. However, while satisfactory agreement with the atomic model can be obtained, the fitting coefficients do not offer a physical explanation for the observed vibrational dependence. In particular, the decrease in A seems puzzling since higher vibrational transitions presumably allow sampling of a greater range of the internuclear coordinate, R_{OO}.

To gain greater physical insight, we turn to an alternative formulation for $\beta(E)$ [36]. The most obvious difference between atomic and molecular anion detachment processes is the presence of internal degrees of freedom. The differential cross section can be written [32]: $d\sigma/d\Omega = (8\pi^3 e^2 \nu/c)\ \langle|\mathrm{T}_{ki}^{v'v''}|^2\rangle$, where e is the electronic charge, ν the photon frequency, and c the speed of light. $\langle|\mathrm{T}_{ki}^{v'v''}|^2\rangle$ is the absolute square of the transition moment between the initial, bound anion and final, neutral molecule + free electron state and (in the absence of rotationally resolved spectra) averaged over all molecular orientations. Within the Franck-Condon approximation, $T_{ki}^{v'v''}$ is factored into vibrational and electronic contributions, giving $\langle|T_{ki}^{v'v''}|^2\rangle = |\int \chi_{v'}\chi_{v''}dR|^2\ \langle|\mathrm{T}_{ki}|^2\rangle$, where χ_v is the vibrational wave function. The problem of predicting or understanding the PAD is one of evaluating the electronic transition matrix element, $T_{ki} = \langle\psi_n;\boldsymbol{k}|\sum \boldsymbol{\varepsilon}_{\mathbf{p}}\cdot\mathbf{r}_i|\psi_a\rangle$. ψ_n, ψ_a are the neutral and anion electronic wave functions and $\mathbf{r}_i$ is the position vector of the i^{th} electron from the center of mass.

If interaction between the parent orbital and all other molecular orbitals is minimal, we can approximate T_{ki} to a one electron integral. This ignores electron-correlation effects but is an instructive approach in evaluating the effect of a specific vibronic transition on the angular distribution. Expanding the continuum wave function $|k\rangle$ and parent orbital in central-potential eigenfunctions and evaluating the angular integrals using the properties of spherical harmonics, it has been shown that the anisotropy parameter can be evaluated using [36]:

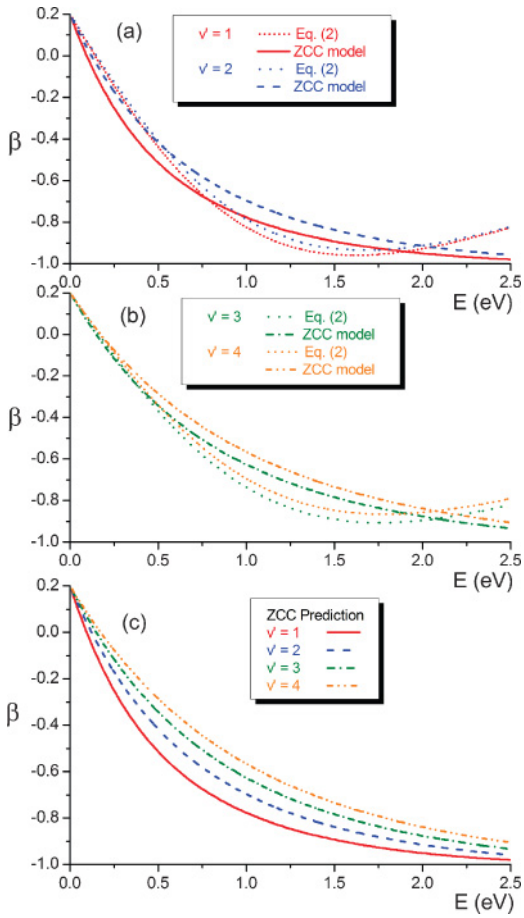

FIG. 3. (Color online) Comparison of ZCC model and experimental results (represented by the fit of (2) to the data). (a) $v' = 1$, 2 (b) $v' = 3$,4. (c) Comparison of the ZCC curves for each transition.

$$\beta(E) = \frac{\sum_{\ell=|\Delta\Lambda|}^{\infty} |C_{n\ell}|^2 (2\ell+1)^{-2}\left[\ell(\ell-1)\left|F_{n\ell}^{E,\ell-1}\right|^2 + (\ell+1)(\ell+2)\left|F_{n\ell}^{E,\ell+1}\right|^2 - 6\ell(\ell+1)\mathrm{Re}\left(F_{n\ell}^{E,\ell-1}F_{n\ell}^{E,\ell+1*}\right)\right]}{\sum_{\ell=|\Delta\Lambda|}^{\infty} |C_{n\ell}|^2 (2\ell+1)^{-1}\left[\ell\left|F_{nl}^{E,\ell-1}\right|^2 + (\ell+1)\left|F_{n\ell}^{E,\ell+1}\right|^2\right]}. \quad (3)$$

In Eq. (3), the $F_{n\ell}^{E,\ell\pm1}$ terms are radial matrix elements, effectively partial-wave detachment cross sections. In the event that the parent orbital is a central-potential eigenfunction, each summation contains a single term and the expression reduces to that of an atomic anion [33,34]. Further approximation ($F_{n\ell}^{E,\ell+1}/F_{n\ell}^{E,\ell-1} \propto E$) yields an expression equivalent to Eq. (2) [35,36].

For O_2^-, we may approximate the π_g orbital as an atomic d orbital. The difference between a purely atomic approach and the molecular case is found in the radial matrix elements, $F_{n\ell}^{E,\ell\pm1} = \int R_{\ell\pm1}(E,r)^*\ r\ R_{n\ell}(r;\ R_{OO})\ r^2\ dr$. The bound electron radial function $[R_{n\ell}(r;\ R_{OO})]$ has a parametric dependence on the internuclear separation, R_{OO}. This can be understood by consideration of the potential energy associated with the anion $X^2\Pi_g$ and neutral $X^3\Sigma_g^-$ states [14,37]. As R_{OO} increases, so does the energy difference between the neutral and anion states, equating to a larger eBE. Increased eBE reduces the spatial volume of the parent orbital, and the radial function falls off more rapidly with r. This is consistent with the idea that the A coefficient in Eq. (2) is related to anion size.

In this context, size is equivalent to the spatial extent of the detachment orbital.

Dramatic changes in the PAD have been observed between different vibronic photoionization bands of the neutral diatomics N_2, CO, and O_2 [4,5]. Such effects are usually associated with resonance phenomena such as autoionizing Rydberg states. In contrast, the variation in $\beta(E)$ for O_2^- detachment is associated with direct detachment. The O_2 anion and neutral difference potential changes rapidly enough that the electronic transition moment varies significantly with R_{OO} [14,37]. Due to the changing overlap of the initial- and final-state vibrational wave functions, each vibronic transition preferentially selects a subset of O_2^- molecular anions with R_{OO} values close to the outer turning points of the neutral O_2 vibrational states. Each vibronic transition is therefore associated with a different range of values of the electronic transition moment.

Previously, only the zero core contribution (ZCC) model has been applied to diatomic anion photodetachment to quantitatively evaluate vibrational effects on the PAD [38]. The approximations applied in the model are similar to those discussed above. The essence of the model is that the excess electron wave function constitutes a detachment orbital which is assumed to be negligible in the "core region," outside which all other orbitals have negligible amplitude. The electronic transition moment integral is then evaluated over the region outside the core. The ZCC predictions of Fig. 3 have been generated using a united atom, *d*-detachment orbital [38]. The experimental data we have presented represent the first systematic test of these predictions. Figure 3 shows that quantitative agreement between the experimental data and the ZCC predictions is not particularly close. However, comparison of the ZCC curves for each v' [Fig. 3(c)] clearly shows that the model predicts a significant dependence on the neutral vibrational state.

Equation (2) predicts a minimum in $\beta(E)$ and the data of Ref. [22] at shorter wavelength shows that this is reproduced experimentally. The ZCC calculation also predicts this minimum but to higher electron kinetic energy. Recent, more sophisticated, computational treatments of O_2^- photodetachment [39–41] (which include electron-correlation effects) also reproduce the minimum. However, these return $\beta(E)$ values that are consistently lower in magnitude than any of the experimental measurements reported here. In addition, these latter calculations completely ignore the effects of vibrational excitation of the neutral O_2. Methodical determination of $\beta(E)$ experimentally demonstrates the importance of the internuclear coordinate in the detachment process. Hopefully, these results will serve as a source on which to base a deeper theoretical understanding of molecular photodetachment processes.

The authors gratefully acknowledge support by the National Science Foundation (grant CHE-0748738) and ANU ARC Discovery Projects grants DP0666267 and DP0880850. We also thank Professor B. J. Orr for discussions regarding treatment of diatomic anion angular distributions.

[1] R. Mabbs *et al.*, Chem. Soc. Rev. **38**, 2169 (2009).
[2] F. Mbaiwa *et al.*, J. Phys. Chem. A **114**, 1539 (2010).
[3] F. Mbaiwa *et al.*, J. Chem. Phys. **132**, 134304 (2010).
[4] T. A. Carlson, Chem. Phys. Lett. **9**, 23 (1971).
[5] T. A. Carlson and A. E. Jonas, J. Chem. Phys. **55**, 4913 (1971).
[6] P. C. Cosby *et al.*, J. Chem. Phys. **63**, 1612 (1975).
[7] P. C. Cosby *et al.*, J. Chem. Phys. **65**, 5267 (1976).
[8] D. S. Burch, S. J. Smith, and L. M. Branscomb, Phys. Rev. **112**, 171 (1958).
[9] D. S. Burch, S. J. Smith, and L. M. Branscomb, Phys. Rev. **114**, 1652 (1959).
[10] R. A. Beyer and J. A. Vanderhoff, J. Chem. Phys. **65**, 2313 (1976).
[11] J. A. Burt, Can. J. Phys. **50**, 2410 (1972).
[12] R. V. Hodges, L. C. Lee, and J. T. Moseley, J. Chem. Phys. **72**, 2998 (1980).
[13] L. C. Lee and G. P. Smith, J. Chem. Phys. **70**, 1727 (1979).
[14] K. M. Ervin *et al.*, J. Phys. Chem. A **107**, 8521 (2003).
[15] R. J. Celotta *et al.*, Phys. Rev. A **6**, 631 (1972).
[16] R. R. Corderman, P. C. Engelking, and W. C. Lineberger, Appl. Phys. Lett. **36**, 533 (1980).
[17] M. J. Travers, D. C. Cowles, and G. B. Ellison, Chem. Phys. Lett. **164**, 449 (1989).
[18] K. M. Ervin and W. C. Lineberger, in *Advances in Gas Phase Ion Chemistry*, edited by N. G. Adams and L. M. Babcock (JAI Press Inc., Greenwich, 1992), Vol. 1, p. 121.
[19] C. G. Bailey *et al.*, J. Chem. Phys. **105**, 1807 (1996).
[20] K. A. Harold *et al.*, Rev. Sci. Instrum. **66**, 5507 (1995).
[21] U. Boesl, C. Bassmann, and R. Kassmeier, Int. J. Mass. Spectrom **206**, 231 (2001).
[22] F. A. Akin, L. K. Schirra, and A. Sanov, J. Phys. Chem. A **110**, 8031 (2006).
[23] A. K. Luong *et al.*, J. Chem. Phys. **114**, 3449 (2001).
[24] K. Le Barbu *et al.*, J. Chem. Phys. **116**, 9663 (2002).
[25] C. Kang *et al.*, J. Chem. Phys. **128**, 104309 (2008).
[26] A. T. J. B. Eppink and D. H. Parker, Rev. Sci. Instrum. **68**, 3477 (1997).
[27] E. W. Hansen and P.-L. Law, J. Opt. Soc. Am. A **2**, 510 (1985).
[28] S. J. Cavanagh *et al.*, Phys. Rev. A **76**, 052708 (2007).
[29] M. Van Duzor *et al.*, J. Chem. Phys. **131**, 204306 (2009).
[30] J. Simons, J. Phys. Chem. A **112**, 6401 (2008).
[31] E. P. Wigner, Phys. Rev. **73**, 1002 (1948).
[32] H. A. Bethe and E. E. Salpeter, *Quantum Mechanics of One- and Two-Electron Atoms* (Springer-Verlag, Berlin, 1957).
[33] J. M. Sichel, Mol. Phys. **18**, 95 (1969).
[34] J. Cooper and R. N. Zare, in *Atomic Collision Processes*, edited by S. Geltman, K. T. Mahanthappa, and W. E. Brittin (Gordon and Breach, New York, 1968), Vol. XI-C, p. 317.
[35] D. Hanstorp, C. Bengtsson, and D. J. Larson, Phys. Rev. A **40**, 670 (1989).
[36] A. D. Buckingham, B. J. Orr, and J. M. Sichel, Philos. Trans. R. Soc. **268**, 147 (1970).
[37] P. H. Krupenie, J. Phys. Chem. Ref. Data **1**, 423 (1972).
[38] R. M. Stehman and S. B. Woo, Phys. Rev. A **23**, 2866 (1981).
[39] P. Lin and R. R. Lucchese, J. Chem. Phys. **114**, 9350 (2001).
[40] C. M. Oana and A. I. Krylov, J. Chem. Phys. **131**, 124114 (2009).
[41] R. R. Lucchese (private communication).